JAR/CUP FO-NR. 71064.2.3 - BRONZE - LATE IRON AGE

Artefact name	Jar/cup FO-Nr. 71064.2.3
Authors	Ingrid González. (HE-Arc CR, Neuchâtel, Neuchâtel, Switzerland) & Valentin. Boissonnas (HE-Arc CR, Neuchâtel, Neuchâtel, Switzerland)
Url	/artefacts/1507/

The object



Credit HE-Arc CR, I.González.

Fig. 1: Jar/cup main body with the fragments of the base,

Description and visual observation

Description of the artefact	Jar/cup (Figs. 1 & 2) developing locally green corrosion products covered with sediments and some organic remains presenting a filiform structure. The object preserves its central cylindric main body. The bottom has been completely detached but several fragments are preserved (Fig. 3). Dimensions: H = 7cm; D = 12cm ; T = 0,3mm. The object comes from a cremation tomb.
Type of artefact	Cup
Origin	Castaneda, Grisons, Switzerland
Recovering date	Excavation 2021, grave 1
Chronology category	Late Iron Age
chronology tpq	500 B.C.
chronology taq	450 B.C.

This work is licensed under CC BY-NC-ND 4.0

Chronology comment	None.
Burial conditions / environment	Soil
Artefact location	Archaeological Service of the Canton of Grisons, Grisons
Owner	Archaeological Service of the Canton of Grisons, Grisons
Inv. number	FO-Nr. 71064.2.3
Recorded conservation data	N/A

Complementary information

None.

Study area(s)



Credit HE-Arc CR, I.González.

Fig. 2: Jar/cup main body with indication of XRF measuring points,



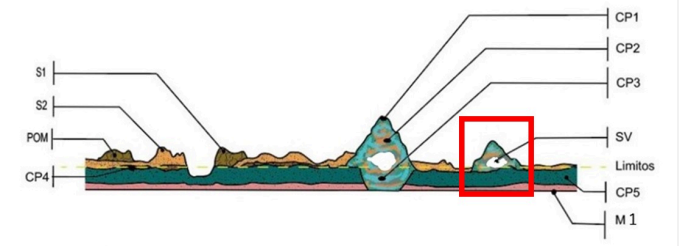
Credit HE-Arc CR, I.González.

Fig. 3: Sampling fragments from the base of the cup,

Binocular observation and representation of the corrosion structure

This work is licensed under CC BY-NC-ND 4.0

The schematic representation below gives an overview of the corrosion structure encountered on the jar/cup from a first visual macroscopic observation.



Layer	Color	Description
S1	Brown	Granular and powdery sediments
S2	Brown	Granular and powdery sediments with strong adhesion to the surface
P.O.M.	Brown	Filiform structure
CP1	Light green	Shiny, hard, dense, adherent corrosion
CP2	Orange	Powdery and loose corrosion
CP3	Light green	Powdery and loose corrosion
SV		Empty space
CP4	Dark brown	Matte and smooth corrosion
CP5	Dark green	Matte and smooth corrosion
M1		Bronze surface

Credit HE-Arc CR, I.González.

Fig. 4: Stratigraphic representation of the corrosion structures of the cup (based on visual observation) with indication of the corrosion structure used to build the MiCorr stratigraphy of Fig. 5 (red rectangular),

MiCorr stratigraphy(ies) – Bi

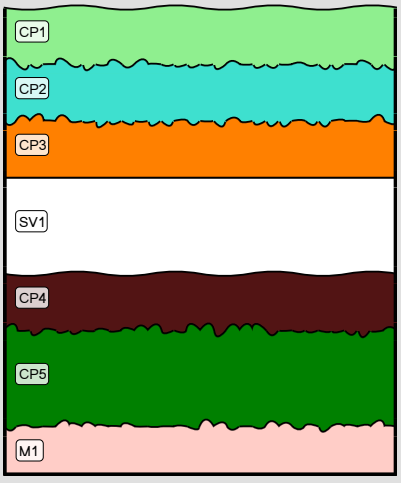


Fig. 5: Stratigraphic representation of the corrosion structure of the cup/jar observed macroscopically under binocular microscope using the MiCorr application. The characteristics of the strata are only accessible by clicking on the drawing that redirects you to the search tool by stratigraphy representation. This representation can be compared to the selected detail of Fig. 4, credit HE-Arc CR, I.González.

Sample(s)

This work is licensed under CC BY-NC-ND 4.0



Fig. 6: Micrograph of the cross-section of a sample taken from the fragments of the base of the cup (Fig. 3) showing the location of Fig. 8, dark field,

Credit HEI Arc, C.Cséfalvay.

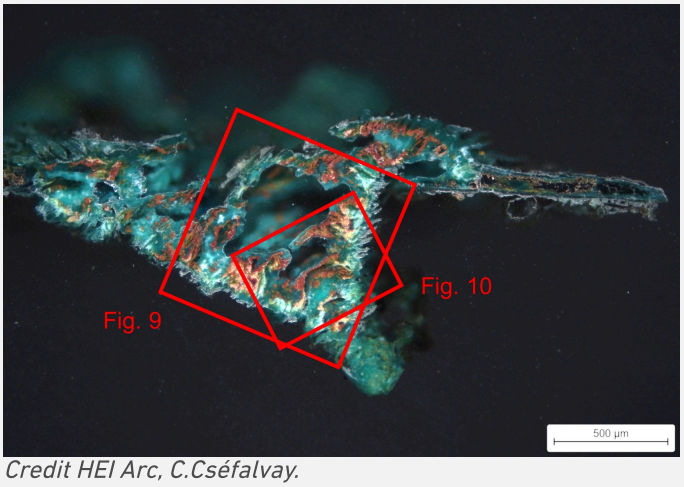


Fig. 7: Micrograph of the cross-section of a sample taken from the fragments of the base of the cup (Fig. 3 and same as Fig. 6) showing the location of Figs. 9 & 10, dark field,

Credit HEI Arc, C.Cséfalvay.

Description of sample	The cross-section corresponds to a fragment detached from the base of the cup/jar (Fig. 3). Its corrosion structure is representative of the corrosion products and the metallic core observed on the whole cup/jar.
Alloy	Bronze
Technology	Hammered, turned and final cold work
Lab number of sample	Tasse_Mag
Sample location	Archaeological Service of the Canton of Grisons, Grisons
Responsible institution	Archaeological Service of the Canton of Grisons, Grisons
Date and aim of sampling	2023, metallography and chemical analyses

Complementary information

None.

Analyses and results

Analyses performed:

Non-invasive approach

- XRF with handheld portable X-ray fluorescence spectrometer (NITON XL3t 950 Air GOLDD+, Thermo

This work is licensed under CC BY-NC-ND 4.0

Fischer®). General Metal mode, acquisition time 60s (filters: Li20/Lo20/M20).

Invasive approach (on the sample)

- Optical microscopy: the sample is embedded in an EPOFIX resin and polished, observed then with a digital microscope KEYENCE VHX-7000 in bright and dark field.

- Metallography: the polished sample is etched with alcoholic ferric chloride and observed by optical microscopy in bright field.

- SEM-EDS: the sample is coated with a carbon layer and analyses are performed on a SEM-FEG JEOL 7001-F equipped with a silicon-drift EDS Oxford detector (Aztec analysis software). Accelerating voltage is of 20 kV and probe current is at about 9 nA. The relative error is considered of about 10% for content range <1mass%, and of 2% for content range of >1mass%.

- FTIR: the sample of a cluster was characterised on a Perkin Elmer System 2000. Spectra were measured in transmission mode at a spectral resolution of 4 cm-1. The sample was flattened on a diamond cell for the analysis.

Non invasive analysis

The XRF analysis of the surface of the cup/jar was carried out on the main body and the handle (Fig. 2). The metal is presumably a copper-tin alloy with some lead, while the light elements detected are from the sediments (Si and Al). The presence of phosphorus (P) could come from human remains from the tomb. There is a very slight presence of titanium (Ti) which could be a kind of contamination.

Elements (wt%)	Cu	Sn	Pb	Ti	Al	P	Si
Main body	41	41	0.5	0.5	7	6	3
Handle	45	24	<0.5	<0.5	15	3	12

Table 1: Results of the XRF analysis of the surface of the cup. Method of analysis: handheld portable X-ray fluorescence spectrometer, HE-Arc CR.

Metal

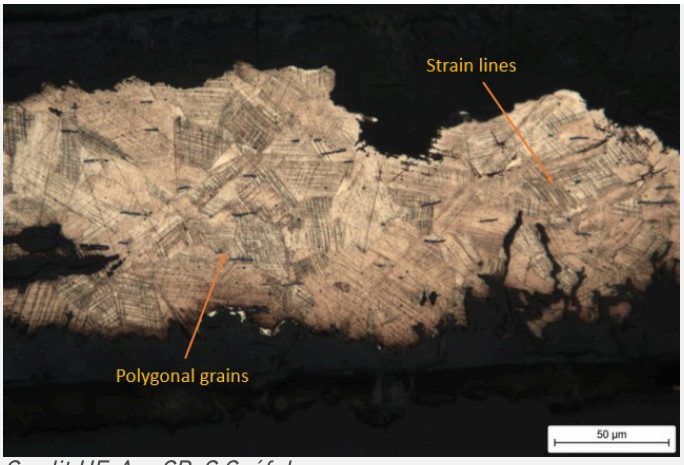
The EDX analysis (Table 2) of the residual metal on cross-section indicates that it is a tin bronze (12 wt% Sn) with a low percentage of lead (0.1 wt% Pb). Clearly the XRF analysis shows a surface enrichment with tin.

The etched metal shows a structure of polygonal grains with strain lines (Fig. 8). This indicates that either the object was submitted to a light annealing process after the intense mechanical work that can be perceived through the slip lines. Or the final mechanical work did not affect the main structure of the grains formed by the previous annealing. Small Pb inclusions are distributed through the sample.

Elements (wt%)	Cu	Sn	Pb
Core metal	88	12	0,1

Table 2: Chemical composition of the core metal. Method of analysis: SEM-EDS.

This work is licensed under CC BY-NC-ND 4.0



Credit HE-Arc CR, C.Cséfalvay.

Fig. 8: Micrograph of the etched cross-section of the sample taken from the fragment of the base of the cup (detail of Fig. 6) in bright field,

Microstructure	Polygonal grains and strain lines
First metal element	Cu
Other metal elements	Sn, Pb

Complementary information

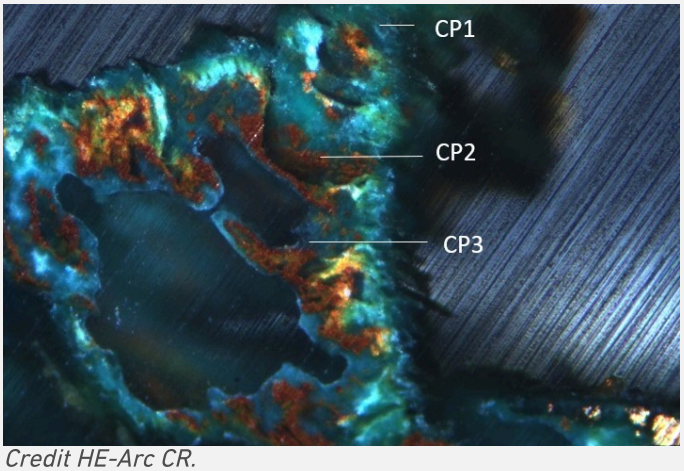
None.

Corrosion layers

The observation of a pustule in cross-section in dark field shows three main corrosion products overlaying each other (Fig. 9). The first green corrosion layer (CP1) possibly corresponds to atacamite ($Cu_2Cl(OH)_3$) as suggested by the FTIR spectrum of Fig. 10. The second corrosion layer inside the pustule (CP2) is probably a copper oxide - cuprite (Cu_2O) and the third light green (CP3) corrosion layer could be malachite ($Cu_2CO_3(OH)_2$), as suggested again by FTIR spectrum of Fig. 12.

The multilayer pustule corrosion has developed similar to the process presented by Formigli (1975) and Scott (2002).

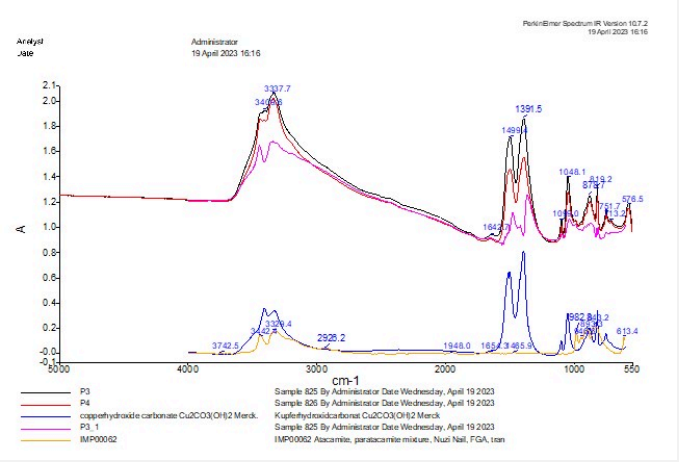
Elemental EDX analysis and mapping (Fig. 10) show phases which are richer in Sn than in Cu. Cl is located in the area closest to the outside of the pustule. Phosphorus (P) is also located in this area, possibly as a soil contaminant in the presence of human remains.



Credit HE-Arc CR.

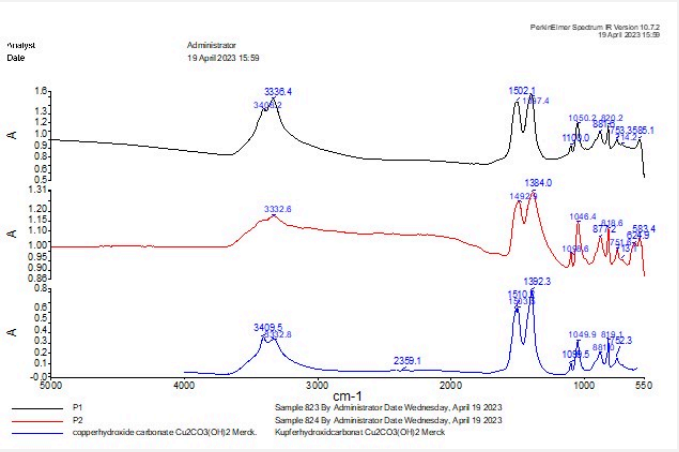
Fig. 9: Micrograph of the metal sample (Fig. 7, rotated by 110°), dark field, showing the location of the multi-layered pustule corrosion,

This work is licensed under CC BY-NC-ND 4.0



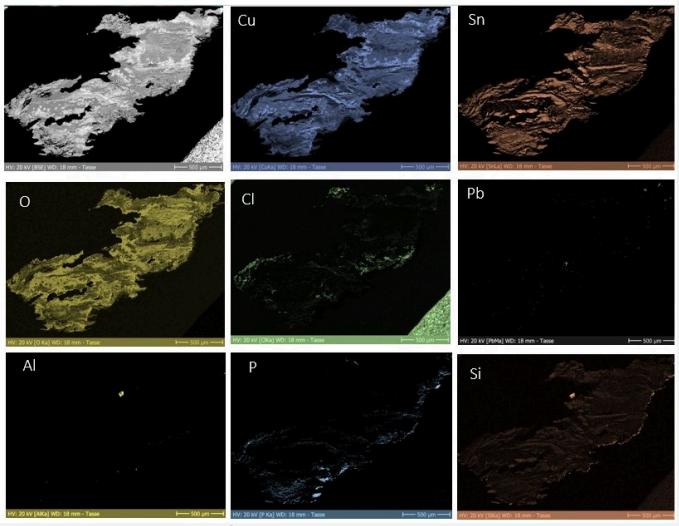
Credit SIK-ISEA, A. Vichi.

Fig. 10: FTIR spectrum of the analysis of a sample from the base of the object Fig. 3, identified as possibly atacamite,



Credit SIK-ISEA, A. Vichi.

Fig. 11: FTIR spectrum of the analysis of a sample from the base of the object Fig. 3, identified as malachite,



Credit HEI Arc, C. Cséfalvay.

Fig. 10: SEM image, BSE-mode, and elemental chemical distribution of the selected area (Fig.7, rotated by 45°),

Corrosion form	Multiform (warty - uniform) - pitting
Corrosion type	Both Formigli (pustules) and type I (Robbiola) otherwise

Complementary information

None.

This work is licensed under CC BY-NC-ND 4.0

MiCorr stratigraphy(ies) – CS

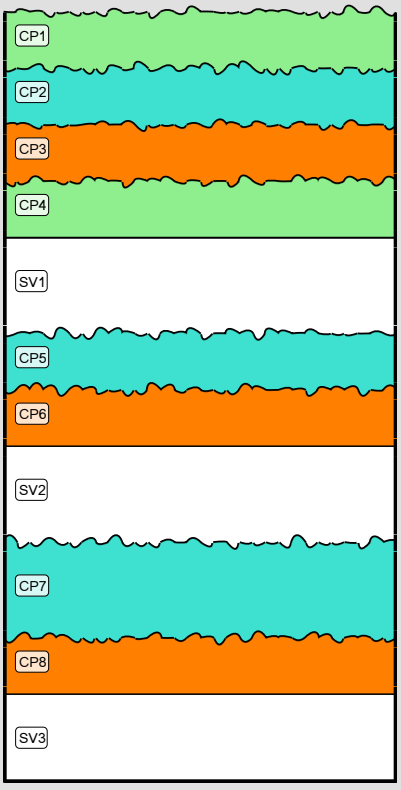


Fig. 13: Stratigraphic representation of the sample taken from the cup/jar in cross-section (dark field) using the MiCorr application. The characteristics of the strata are only accessible by clicking on the drawing that redirects you to the search tool by stratigraphy representation. This representation can be compared to fig. 9, Credit HE-Arc CR, I. González.

Synthesis of the binocular / cross-section examination of the corrosion structure

The stratigraphies obtained by binocular and cross-section observation show a few differences that can be attributed to the different scales of observation and the impossibility to visualise both a pustule and the remaining metal underneath. Under binocular microscope, it is difficult to differentiate the multiple strata of the pustule. Only the main strata are indicated.

Under cross-section, the distribution of strata appears more clearly while this distribution and succession of strata are different in the middle of the pustule versus its edges. CP4 is similar to CP1, while CP5/CP7 are similar to CP2 and CP6/CP8 are similar to CP3.

CP4 and CP5 of the Bi stratigraphy do not show up on the CS stratigraphy. Similarly the M1 stratum is not described.

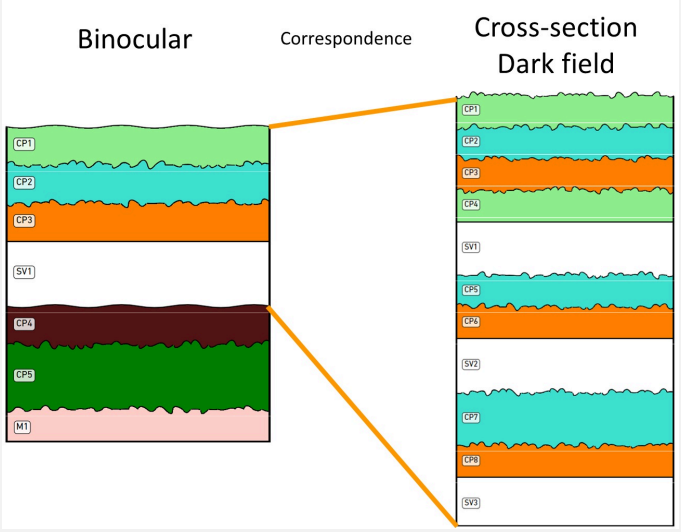


Fig. 14: Stratigraphic representation side by side of binocular view and cross-section (dark field),

This work is licensed under CC BY-NC-ND 4.0

Credit HE-Arc CR, I. González.

Conclusion

The jar/cup is made of a tin bronze with Pb inclusions. Metallographic observation of the remaining metal revealed a polygonal grain structure with strain lines. This indicates that the metal was annealed and cold worked several times, with a final cold working. The metal is in an advanced state of mineralisation with the formation of pustules crossing the full thickness of the metal.

Observation of the corrosion layers showed a typical corrosion structure for an archaeological bronze. The main corrosion products found are malachite and most likely cuprite and atacamite. The object shows a Sn enrichment process on the surface. The presence of P can be attributed to the presence of human remains in the grave, while the presence of Si, Al and Ti is mainly due to the elements of the burial soil.

The limit of the original surface limit corresponds to the upper surface of the brown and dark green layer. The corrosion is multiform type I according to Rabbiola (1998) while the pustules are of the Formigli type (Formigli 1975).

References

References on object and sample

1. González, I. (2023) Tasse FO-Nr. 71064.2.3, Archaeological Service of the Canton of Grisons, rapport d'intervention. Haute Ecole ARC, Neuchâtel, non-publié.
2. MiCorr_Fragments of oenochoe GV132-01/US26-OBJ.10.
3. González, I. (2023) Jar/cup - Bronze - Late Iron Age, FO-Nr. 71064.2.3, MiCorr, Switzerland, Haute Ecole ARC, Neuchâtel, non-publié.

References on analytic methods and interpretation

4. Formigli, E. (1975) « Die Bildung von Schichtpocken auf antiken Bronzen ». In ArbeitsblätterAdR, Gruppe 2, 51-58.
5. Robbiola, L. (1998) Morphology and mechanisms of formation of natural patinas on archaeological Cu-Sn alloys. In Corrosion Science, 40, 12, 2083-2111.
6. Scott, D. A. (2002) Copper and bronze in Art, corrosion, colorants, conservation. Getty publications, Los Angeles.
7. Scott, D. A. (1991) Metallography and microstructure of ancient and historic metals. Getty publications, Los Angeles.

This work is licensed under CC BY-NC-ND 4.0